

A COMPARISON OF RADIATION BOUNDARY CONDITION STRATEGIES FOR HELMHOLTZ EQUATIONS

Catherine Piellusch-Castle^{*1}, Yin-shang Liu², Bernd Lichtenberg², Douglas B. Meade¹, and Kevin J. Webb²

¹ Department of Mathematics, University of South Carolina, Columbia, SC 29208, USA
Telephone: (803) 777-6183; FAX: (803) 777-3783; e-mail: meade@math.sc.edu

² School of Electrical Engineering, Purdue University, W. Lafayette, IN 47907, USA
Telephone: (317) 494-3373; FAX: (317) 494-6440; e-mail: webb@ecn.purdue.edu

1. Introduction. Many problems in electromagnetics involve the solution of a wave equation in an exterior domain. The unbounded computational domain complicates the search for efficient numerical solution techniques. A number of different solutions to this problem have been proposed, studied, and implemented; an excellent summary is the review article by Givoli [2]. A feature common to many of these procedures is the approximate reformulation of the problem on a bounded domain with a circular artificial boundary. Numerical solutions to these problems are then easily obtained by, e.g., the finite element method.

In this paper we consider a number of radiation boundary conditions (RBCs). In particular, we present a procedure that can be used to extend any boundary condition for a circular boundary to a general convex curve *without unduly complicating the numerical implementation*. It is this last point that is most important. Whereas a simple change of variables suffices to provide an exact boundary condition on the more general curve, the resulting boundary condition is not appropriate for numerical implementation. We present a simple, yet general, procedure for finding an approximate boundary condition that is suitable for numerical computations.

Following a brief discussion of the problem on the unbounded domain, we present, in Section 3.1, several approximate reformulations of this problem on a bounded domain with circular artificial boundary. Section 3.2 contains the description of our procedure for generalizing these for other artificial boundaries. Computational comparisons of different RBCs are presented in Section 4.

In-depth descriptions of the techniques used in this paper can be found in [7], [8] and the references therein.

2. Original Problem and Reformulations. We consider the problem of finding the scattered wave produced when an incident wave is reflected from a scatterer. Assuming the incident field is time-harmonic, with temporal dependence $e^{-i\omega t}$, the goal is to solve

$$\begin{aligned} (1) \quad & \Delta u + k^2 u = 0 \quad \text{in } \Omega^+ \\ (2) \quad & u = g \quad \text{on } \Gamma, \\ (3) \quad & \lim_{r \rightarrow \infty} r^{1/2}(u_r - iku) = 0 \quad \text{uniformly in } \theta \end{aligned}$$

where Γ is the boundary of the scatterer, Ω^+ is the (unbounded) exterior of the scatterer, and g is obtained from the incident wave.

Equation (3) is the Sommerfeld radiation condition. This “boundary condition at infinity” ensures that the boundary-value problem is well-posed; in particular that the solution is unique. Physically, this condition states that any solution is outgoing.

The basic idea for the reformulation on a bounded domain is to introduce an *artificial boundary*, Γ^t , and solve a new problem on Ω^t , the truncated domain. This leads to the boundary value problem

$$\begin{aligned} (4) \quad & \Delta u + k^2 u = 0 \quad \text{in } \Omega^t \\ (5) \quad & u = g \quad \text{on } \Gamma, \\ (6) \quad & \mathcal{B}u = 0 \quad \text{on } \Gamma^t, \end{aligned}$$

where \mathcal{B} is an, as yet unspecified, artificial boundary operator.

3. Artificial Boundary Conditions. The artificial boundary condition, (6), must play the same role as the radiation condition, without introducing spurious reflections. In principle an exact reformulation does exist. However, the exact boundary operator is defined in terms of the solution of an integral equation. This, combined with the fact that the boundary operator is non-local, complicates the computational implementation of this reformulation.

3.1. Circular Artificial Boundary. A common form for approximate RBCs on a circle is

$$(7) \quad \mathcal{B}u = u_r - \alpha(\tau)u - \beta(\tau)u_{\theta\theta}.$$

Note that this is a local condition. Moreover, implementation of this boundary condition in a variational (FEM) method is very natural.

Selection of the coefficients α and β is often based on an expansion of the solution in the exterior of a circle. A sequence of approximate RBCs, $\{\mathcal{B}_n\}$, can be constructed from the boundary operators that annihilate the first m terms in the expansion. Two examples are the Bayliss-Turkel RBCs [1], based on the far-field expansion

$$(8) \quad u = \frac{e^{-ikr}}{\sqrt{r}} \sum_{n=0}^{\infty} \frac{a_n(\theta)}{r^n}$$

and the Li-Cendes RBCs [4], which are based on the Hankel expansion $u = \sum_{n=0}^{\infty} b_n(\theta)H_n(kr)$, where H_n is the n^{th} -order Hankel function of the second kind. A third set of coefficients, the Mittra-Ramahi RBCs [5] are simply the $O(r^3)$ expansions of the BT RBCs. The coefficients for the first- and second-order RBCs for all three of these methods are listed in Table 3.1.

3.2. General Artificial Boundary. When the artificial boundary is not a circle, (7) is no longer valid. Several authors have proposed methods for converting (7) into an RBC expressed in terms of normal (ν) and tangential (τ) derivatives on the artificial boundary. Two examples are i) using the substitutions $\frac{\partial}{\partial r} \mapsto \frac{\partial}{\partial \nu}$, $\frac{1}{r} \mapsto \kappa$, and $\frac{1}{r} \frac{\partial}{\partial \theta} \mapsto \frac{\partial}{\partial \tau}$ and ii) using an approximate change of coordinates from (r, θ) to (ν, τ) . While these do lead to RBCs in a convenient form, both procedures impose additional approximations that are not necessary and may not be appropriate.

An exact translation of (7) into normal (ν) and tangential (τ) coordinates yields the boundary operator

$$(9) \quad \mathcal{B}u = Au + Bu_{\tau} + Cu_{\nu} + Du_{\tau\tau} + Eu_{\tau\nu}$$

where $A = \alpha - k^2\beta(n_{\theta})^2$, $B = -t_r + \beta t_{\theta\theta}$, $C = -n_r + \beta(n_{\theta\theta} - \kappa(n_{\theta})^2)$, $D = \beta((t_{\theta})^2 - (n_{\theta})^2)$, $E = 2\beta t_{\theta}n_{\theta}$. The mixed derivative term, $u_{\tau\nu}$, complicates the implementation of this boundary condition in a variational method. In [8] the tangential derivative of the first-order RBC is used to obtain an approximation to $u_{\tau\nu}$ in terms of u , u_{τ} , u_{ν} , and $u_{\tau\tau}$. Even though the resulting linear system will not be symmetric, this RBC is easy to implement in a FEM.

4. Comparison of Approximate RBCs. Two tests are used to illustrate the effects of the approximations used in the different RBCs. The results of these tests confirm that the proposed procedure produces effective approximate RBCs on non-circular artificial boundaries.

Given a (smooth) artificial boundary, γ , and a function u , the error due to the approximate RBC is $|u_{\nu} - \mathcal{B}u|$. Figure 2 displays this information for the case when $u = H_0(r)$ and γ is an ellipse. The solid line is the exact second-order BT RBC. In both cases it is clear that, averaged over the entire boundary, the new RBC (labelled MPW via RC) is the best approximation to the second-order BT RBC.

Suppose the scatterer is a long, thin perfect electric conductor (pec) slab as in Figure 1. Truncating the computational domain with a circular artificial boundary will still result in a large computational domain. The size of the computational domain can be greatly reduced through the use of a ‘‘capped strip’’ artificial boundary. Numerical experiments illustrate that the computed solutions found using the approximate RBCs on a general boundary are comparable to the solution computed using the circular artificial boundary. The magnitude of the solutions computed using a circular and a capped strip boundary are displayed in Figure 3.

In fact, the solutions obtained from smaller domains are not much worse; however, the computational domain is so small that graphical comparisons are not practical. Some statistics comparing the quality of solutions and computational effort are summarized in Table 2. Note that all comparisons are made relative to the computed solution on the circular domain. Additional computation results can be found in [7] and [8].

Type	α_1	β_1	α_2	β_2
Bayliss-Turkel	$-(ik + 1/2r)$	0	$-ik - 1/2r + 1/8r(1 + ikr)$	$1/2r(1 + ikr)$
Li-Cendes	$-\frac{kH_1(kr)}{H_0(kr)}$	0	$-k^2r(g_2(kr) - 1)/(kr g_1(kr) - 1)$	$1/(kr g_1(kr) - 1)$
Mittra-Ramahi	$-(ik + 1/2r)$	0	$-ik - 1/2r - i/8kr^2 + 1/8k^2r^3$	$-i/2kr^2 + 1/2k^2r^3$

TABLE 1. Coefficients of first- and second-order RBCs for a circular boundary. (The functions g_1 and g_2 which appear in the second-order Li-Cendes coefficients are rational functions of H_0 , H_1 and their first two derivatives [4].)

Comparison of Boundary Geometries

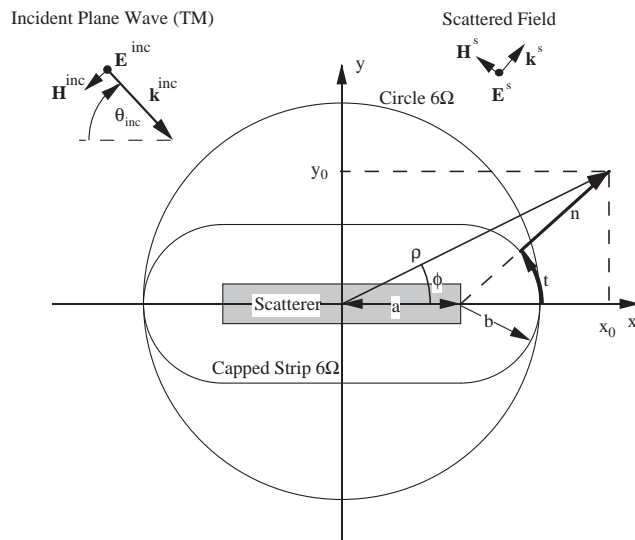


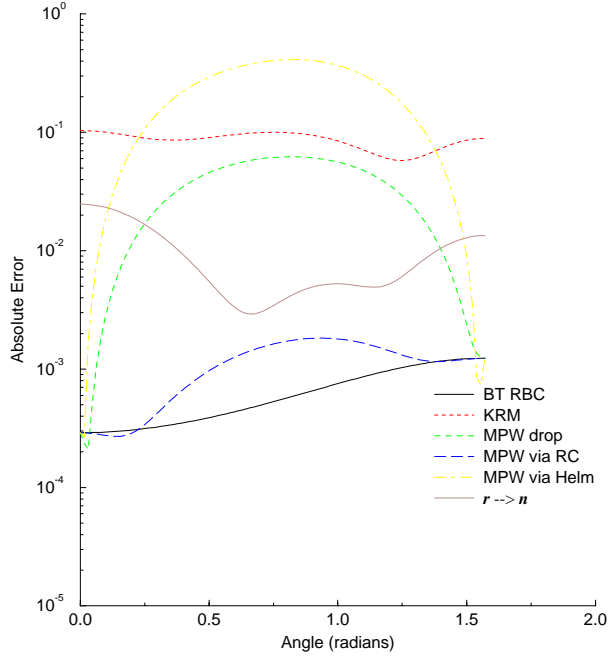
FIGURE 1. Comparison of computational domains for a thin rectangular scatterer for a circular and a capped strip artificial boundary. Note the definition of θ .

Domain	$\frac{\text{Area}}{\lambda^2}$	Area Savings	# Unknowns	Total Time (s)	Time Savings	Relative L_2 Error
Circle ($r=5$)	77.93		36,818	2,724.99		
CS ($b=2.0$)	35.97	53.8%	17,062	566.91	79.2%	4.75%
CS ($b=1.5$)	24.47	53.8%	11,650	254.88	90.6%	8.99%
CS ($b=1.0$)	14.54	81.3%	7,012	88.64	96.7%	15.33%
CS ($b=0.5$)	6.19	91.0%	3,064	17.33	99.4%	35.00%

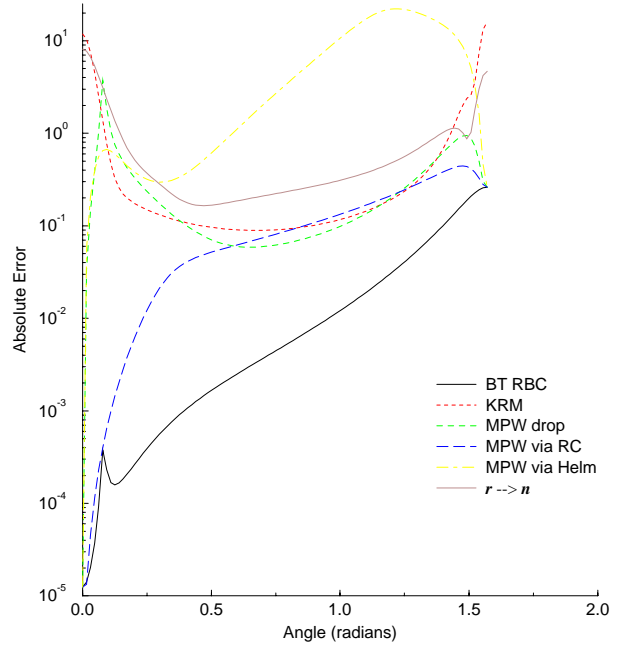
TABLE 2. Comparison of geometrical properties of domains, computational effort, and accuracy for a circular domain (using the second-order BT RBC) and four different capped strip domains (using the generalized BT RBC obtained via the differentiated first-order BT RBC). All CPU timings were performed on an Ardent P3 with 4 processors and no optimization. The errors are relative errors computed against the solution on the circular domain.

REFERENCES

- [1] A. Bayliss, M. Gunzburger, E. Turkel, “Boundary conditions for the numerical solution of elliptic equations in exterior regions”, *SIAM J. Appl. Math.*, 42(1982), pp. 430–451.
- [2] D. Givoli, “Non-reflecting boundary conditions”, *J. Comput. Phys.*, 94(1991), pp. 1–29.
- [3] J. M. Jin, *The Finite Element Method in Electromagnetics*, John Wiley & Sons, New York, NY, 1993.
- [4] Y. Li, Z. J. Cendes, “Modal expansion absorbing boundary conditions for two-dimensional electromagnetic scattering”, *IEEE Trans. Magnetics*, 29(1993), pp. 1835–1838.
- [5] A. Khebir, O. Ramahi, R. Mittra, “An efficient partial differential equation technique for solving the problem of scattering by objects of arbitrary shape”, *Microwave and Optical Tech. Lett.*, 2(1989), pp. 229–233.
- [6] G. A. Kriegsmann, A. Taflove, K. R. Umashankar, “A new formulation of electromagnetic wave scattering using an on-surface radiation boundary condition approach”, *IEEE Trans. Antennas and Propagation*, 35(1987), pp. 153–161.
- [7] B. Lichtenberg, J. S. Reynolds, K. J. Webb, A. F. Peterson, D. B. Meade, “Numerical study of a conformable two-dimensional radiation boundary condition”, *IEEE Trans. Antennas and Propagation*, submitted.
- [8] D. B. Meade, G. W. Slade, A. F. Peterson, K. J. Webb, “Comparison of local radiation boundary conditions for the scalar Helmholtz equation with general boundary shape”, *IEEE Trans. Antennas and Propagation*, submitted.

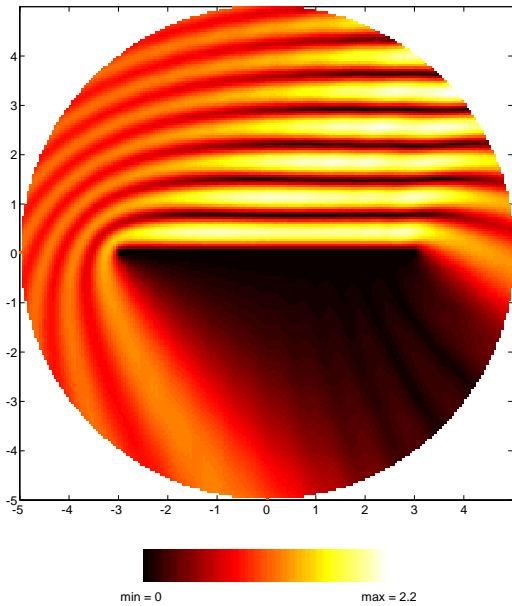


a) 3×2 ellipse

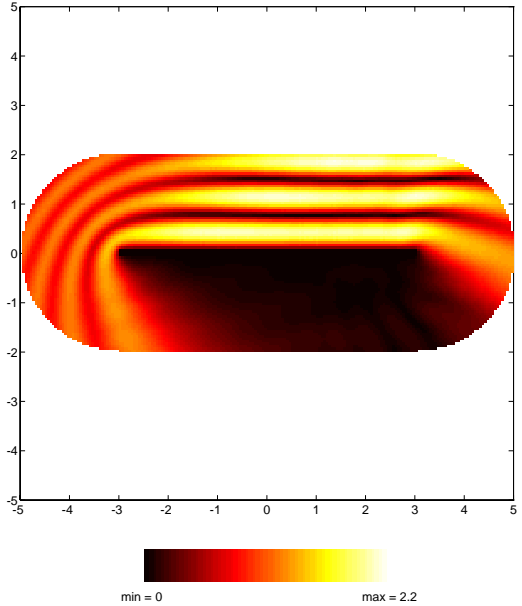


b) 3×0.25 ellipse

FIGURE 2. Comparison of RBCs for the scalar Helmholtz equation with $k = 1$ for two different ellipses. The absolute error is $|u_\nu - \mathcal{B}u|$ where $u(r, \theta) = H_0(r)$. (An $a \times b$ ellipse has semi-axes a and b and center $(0, 0)$ where $a \cong \frac{a}{2\pi}\lambda$.)



a) circular boundary ($r = 5$)



b) capped strip ($b = 2$)

FIGURE 3. Computed magnitude of E_z from TM polarization. The scatterer is a $(6 \times 0.1)\lambda$ pec slab; the incident field is a plane wave with $\theta = 45^\circ$.